ISSN 0023-1584, Kinetics and Catalysis, 2019, Vol. 60, No. 2, pp. 155–163. © Pleiades Publishing, Ltd., 2019.
Russian Text © R.L. Safiullin, E.M. Chainikova, A.N. Teregulova, S.L. Khursan, 2019, published in Kinetika i Kataliz, 2019, Vol. 60, No. 2, pp. 171–180.

Kinetics and Mechanism of the Reactions of Aromatic Nitroso Oxides with Tetracyanoethylene

R. L. Safiullin[a], E. M. Chainikova[a], *, A. N. Teregulova[a], and S. L. Khursan[a]
[a] *Ufa Institute of Chemistry, Russian Academy of Sciences, Ufa, Bashkortostan, 450054 Russia*
**e-mail: kinetic@anrb.ru*

Received July 31, 2018; revised November 6, 2018; accepted November 14, 2018

Abstract—The kinetics of reaction of phenylnitroso oxide and a number of its *para*-substituted analogues (R = Me_2N, MeO, Me, and Br) with tetracyanoethylene in acetonitrile at room temperature was studied using flash photolysis. It was established that nitroso oxides exhibited nucleophilic properties in this reaction, and the rate constants for the *trans* forms of these species in the above series changed by seven orders of magnitude. In the presence of a strong electron-donating substituent (Me_2N or MeO), the *cis* form, which is usually inert toward organic substrates, also reacted with the olefin along with the *trans* form. The reaction mechanism was studied using the density functional theory.

Keywords: aromatic nitroso oxides, tetracyanoethylene, kinetics, flash photolysis, quantum-chemical modeling
DOI: 10.1134/S0023158419020095

INTRODUCTION

Aromatic nitroso oxides (ArNOO) are formed as *cis* and *trans* isomers by the reaction of triplet nitrenes with molecular oxygen [1, 2]. The *trans* forms of these species manifest activity toward organic substrates. In reaction with aromatic phosphines, they behave like typical electrophiles; that is, electron-donating substituents in a phosphine molecule and electron-withdrawing substituents in a nitroso oxide molecule increase the reaction rate constant [3]. The ambiphilic nature of nitroso oxides was detected in reaction with *para*-substituted styrenes, when electron-donating and electron-withdrawing substituents in the olefin molecule led to an increase in the rate of reaction compared to unsubstituted styrene; that is, the Hammett functions were V-shaped [4].

In this work, we studied the kinetics of the reaction of nitroso oxides **IIa**–**IIe** (generated from corresponding azides **Ia**–**Ie**) with an electron-deficient olefin (tetracyanoethylene) in acetonitrile at room temperature by flash photolysis and investigated the reaction mechanism using density functional theory methods.

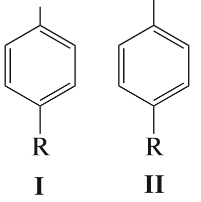

I **II**

a: R = H
b: R = NMe_2
c: R = OMe
d: R = Me
e: R = Br

EXPERIMENTAL

Reagents

Acetonitrile and hexane for HPLC (Cryochrom) and tetracyanoethylene (TCE) (Lancaster) were used without further purification. Azides **Ia**, **Id** [5], **Ib**, **Ic**, and **Ie** [6] were synthesized according to published procedures. Compounds **Ia** and **Id** were distilled under vacuum and **Ic** and **Ie** were recrystallized from hexane and ethanol, respectively. Compound **Ib** was purified by column chromatography on silica gel 60 (Merck; eluant, hexane/ethyl acetate (2–3 vol %)).

Kinetic Measurements

Kinetic studies were performed on a flash photolysis system, the parameters of which were given elsewhere [7]. An IFP 5000-2 lamp served as a photolytic source (the maximum pulse energy was 400 J at a voltage of 5 kV and a capacitance of 32 μF; ~90% light energy was emitted in 50 μs). The spectrophotometric part of the system consisted of a source of continuous probe radiation (a DKSSh-150 xenon lamp with a system of quartz lenses and diaphragms for forming a probe beam), an MDR-4 monochromator, an FEU-97 photomultiplier tube, and a C9-8 storage oscilloscope. This system was supplemented by a device for the computer processing of pulse signals. The signal from the photomultiplier tube was amplified after the precompensation of a constant component and fed to the input of the digital oscilloscope, which operated in standby mode. The oscilloscope allowed us to store a signal (2048 points) with a minimum time resolution of 50 ns and a voltage resolution of 256 levels. The digitized signal was transferred to the computer through a CPC interface (IEEE-488, GPIB). The hardware part of the interface on the computer side was made based on standard parallel ports used in bidirectional EPP/ECP mode. All interface functions were implemented in the PASCAL language. The signal-processing program automatically determined (with manual adjustment) the beginning and the end of a light pulse and zero optical absorption. The kinetic curves were processed using nonlinear regression analysis. Error in the determination of rate constants was no greater than 10%. A thermostatically controlled quartz cell with an optical path length of 10 cm and an inner diameter of ~1 cm served as a reactor. The flash photolysis of arylazide solutions in acetonitrile or hexane saturated with atmospheric oxygen was carried out with filtered light (a UFS-2 optical filter; transmission band, λ = 270–380 nm). The initial concentration of azides was 2.5×10^{-4} mol/L.

Quantum-Chemical Simulation

All of the calculations were performed using the M06L density functional [8] and the 6-311+G(d,p) polarized split valence triple basis set [9, 10]. The quantum-chemical calculations were performed on a cluster supercomputer at the Ufa Institute of Chemistry, Russian Academy of Sciences using the Gaussian 09, Revision C.1 software package [11]. The IEFPCM polarized continuum model [12] was used to describe solvation effects. The full optimization of the geometric parameters was performed for all structures, complexes, and transition states, and the Hessian matrix of second-order partial derivatives was calculated to judge the nature of a stationary point in the potential energy surface (PES) of the system under studied. Stable structures were characterized by the absence of negative elements in the diagonalized Hessian matrix, and the transition states were characterized by the presence of the only negative element. The absolute values of the Gibbs free energies of the structures studied were found in the form of the sum of the total energy, the energy of zero oscillations, and a thermal correction to the Gibbs energy ($G^{\circ}_{298\text{ K}} - U^{\circ}_{0\text{ K}}$). In the calculation of the thermodynamic parameters of the complexes of arylnitroso oxides with TCE, we took into account the error of the superposition of BSSE basis sets using a counterweight method [13].

RESULTS AND DISCUSSION

General Reaction Scheme

The photolysis of the solutions of azides **Ia**–**Ie** under the experimental conditions described above led to the generation of corresponding nitroso oxides **IIa**–**IIe** as two isomeric forms (Scheme 1). The optical spectra of the *cis* and *trans* isomers of the nitroso oxides were consistent with those published previously [2].

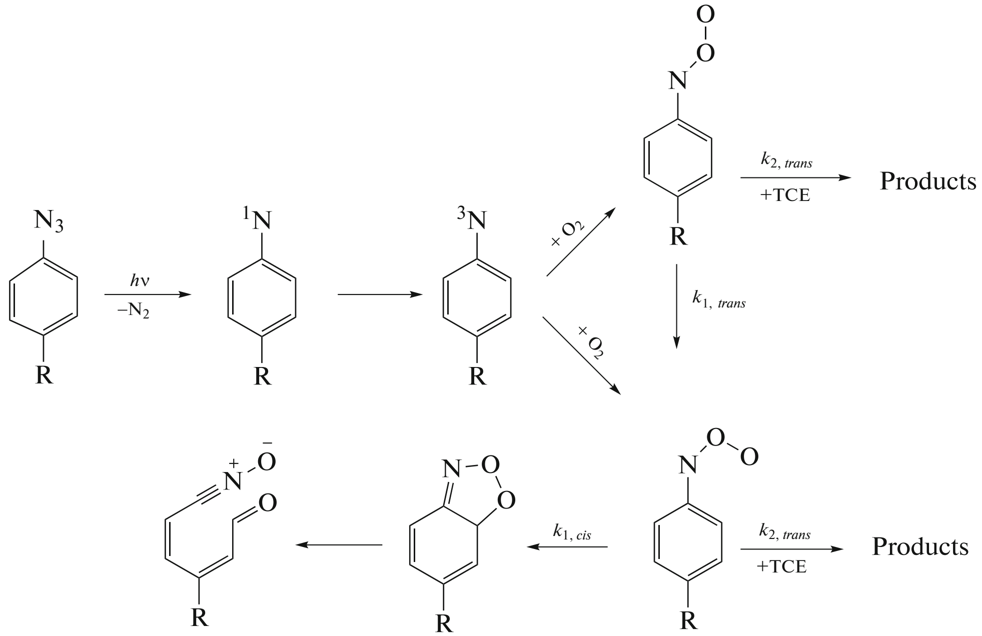

Scheme 1.

The decay of both isomeric forms of ArNOO is carried out by a first-order reaction with rate constants k_1, which differ for the *cis* and *trans* forms of ArNOO (Scheme 1, Table 1). Previously, on a number of examples, it was shown that *cis*-ArNOO undergoes a so-called *ortho*-cyclization reaction, whereas the con-

Table 1. Rate constants of the unimolecular decay of the isomeric forms of nitroso oxides and their reaction with TCE (acetonitrile, $T = 295 \pm 2$ K)

4-R-C_6H_4-NOO	Isomer	k_1, s^{-1}	k_2, L mol^{-1} s^{-1}
R = Me_2N (**IIb**)	*cis*	150 ± 5	$(3.1 \pm 0.1) \times 10^9$
	trans	260 ± 10	$(3.3 \pm 0.3) \times 10^9$
R = MeO (**IIc**)	*cis*	11.3 ± 0.2	$(2.66 \pm 0.04) \times 10^6$
	trans	0.37 ± 0.02	$(5.0 \pm 0.4) \times 10^5$
R = Me (**IId**)	*cis*	2.25 ± 0.06	–
	trans	0.17 ± 0.01	$(3.9 \pm 0.1) \times 10^3$
R = H (**IIa**)	*cis*	1.19 ± 0.06	–
	trans	0.10 ± 0.01	$(3.2 \pm 0.2) \times 10^3$
R = Br (**IIe**)	*cis*	1.45 ± 0.02	–
	trans	0.14 ± 0.01	$(4.1 \pm 0.2) \times 10^2$

formational conversion of the *trans* isomer into the *cis* form is the main channel of its consumption (Scheme 1). When adding TCE to the reaction system, the lifetime of the observed species decreased inversely the added olefin concentration. This fact indicates the occurrence of nitroso oxide reactions with TCE characterized by bimolecular rate constant k_2 (Scheme 1). Note that it is likely that the *cis* isomers of nitroso oxides **IIa**, **IId**, and **IIe** are not involved in the reaction because the lifetime of these species is insensitive to the addition of TCE.

Flash Photolysis

In the absence of oxidized substrates, the kinetic curves of the absorption decay measured under flash photolysis of the solutions of azides **Ia** and **Ic**–**Ie** in the presence of oxygen in the wavelength region where both isomers of the corresponding nitroso oxides absorbed had a biexponential character and were described by the five-parameter equation

$$A = A_\infty + A_0^{\mathrm{I}} e^{-k_{1,\,cis} t} + A_0^{\mathrm{II}} e^{-k_{1,trans}\, t}, \quad (1)$$

where $A_\infty + A_0^{\mathrm{I}} + A_0^{\mathrm{II}} = A_0$ is the initial optical absorption of nitroso oxide, $k_{1,cis}$ and $k_{1,trans}$ are the rate constants of the consumption of the *cis* and *trans* isomers, respectively, and A_∞ is the final optical absorption due to the absorption of reaction products.

The absorption maximums of the *cis* and *trans* isomers of nitroso oxide **IIb** in acetonitrile were very different (500 and 600 nm, respectively). At these wavelengths, only one of the two isomers absorbed; therefore, the kinetics of the consumption measured at either of them was described by the simple unimolecular equation

$$A = A_\infty + (A_0 - A_\infty)\, e^{-k_{\mathrm{eff}} t}. \quad (2)$$

In the absence of TCE additives, $k_{\mathrm{eff}} = k_{1,cis}$ or $k_{1,trans}$ depending on the monitoring wavelength.

Table 1 summarizes the unimolecular-reaction rate constants of the decay of the nitroso oxide isomers in acetonitrile, which were measured previously [14]. With the exception of **IIb**, the rate constant of the consumption of the *cis* isomers was greater by an order of magnitude or more than the corresponding value for the *trans* isomers of ArNOO. In the case of nitroso oxides **IIa**, **IId**, and **IIe**, when adding tetracyanoethylene to the system under study the kinetic curves of the absorption decay became monoexponential and were described by Eq. (2). This can be explained by the fact that the effective rate constant of the consumption of the *trans* isomer increased and approached the analogous value for the *cis* isomer, on which additives of olefin did not exert a noticeable effect. As a result, the two species became kinetically indistinguishable. To avoid distortion of the results, the reaction kinetics of the *trans* isomers of the above nitroso oxides with tetracyanoethylene was studied at the wavelength of 440 nm, at which the *cis* isomers did almost not absorb.

Figure 1 shows the dependences of the effective rate constants of the consumption of the *trans* forms of nitroso oxides **IId** and **IIe** on the concentration of tetracyanoethylene, $k_{\mathrm{eff}} = k_1 + k_2[\mathrm{TCE}]$. The absolute values of the rate constants of the studied reaction were obtained from the slopes of these dependences (Table 1).

In the case of nitroso oxides **IIb** and **IIc** with strong electron-donating substituents in the presence of TCE, the rate of the consumption of both isomeric forms increased. Figure 2 shows the kinetic curves of the consumption of nitroso oxide **IIc** in the absence of the additive (curve *1*) and in the presence of 3.75×10^{-4} mol/L TCE (curve *2*) and their theoretical description by Eq. (1). The kinetics of the reaction of nitroso oxide **IIb** with tetracyanoethylene was monitored at the wavelengths of 500 nm (*cis* isomer) and 600 nm (*trans* isomer). The kinetic curves were treated by Eq. (2). Thus, we obtained the linear dependences of the effective rate constants of the consumption of the isomeric

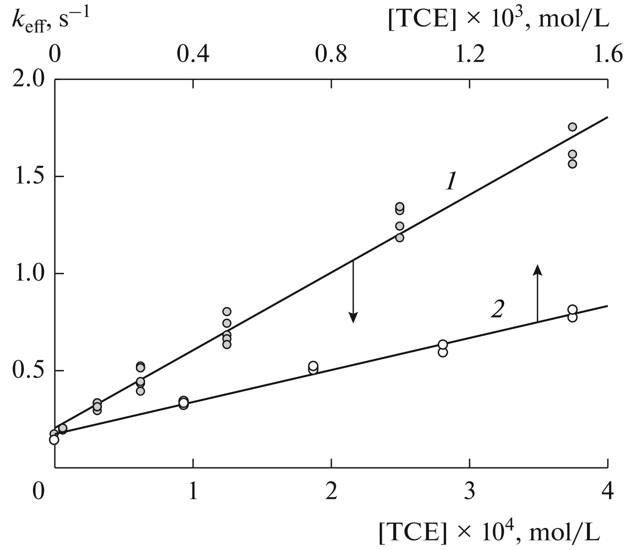

Fig. 1. Dependence of the effective rate constants of the consumption of the *trans* isomers of nitroso oxides (*1*) **IId** and (*2*) **IIe** on the concentration of TCE. Experimental reaction conditions: acetonitrile, $T = 295 \pm 2$ K, and the detection wavelength of 440 nm.

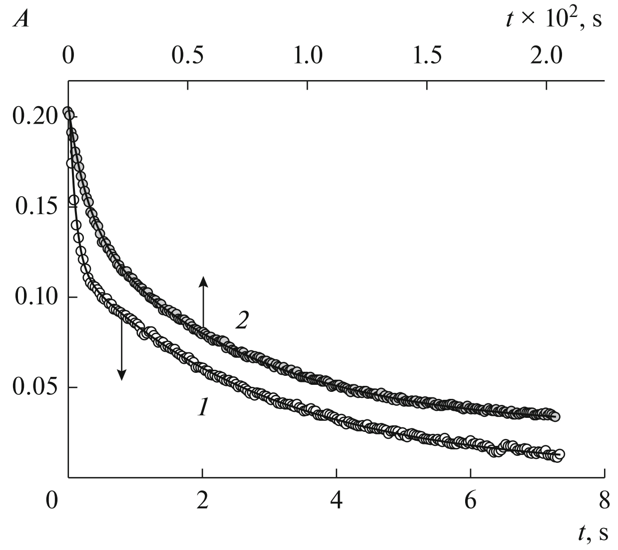

Fig. 2. Kinetic curves of the absorption decay of nitroso oxide **IIc** and their description by Eq. (1) (solid lines): (*1*) in the absence of TCE and (*2*) at [TCE] = 3.75×10^{-4} mol/L. Experimental reaction conditions: acetonitrile, $T = 295 \pm 2$ K, and the detection wavelength of 440 nm.

forms of nitroso oxides **IIb** and **IIc** on the TCE concentration and calculated the absolute rate constants of the reaction under study (Table 1).

As follows from the data of Table 1, the substituent at the *para* position of nitroso oxide exerts a tremendous effect on the reactivity of these species toward tetracyanoethylene. The rate constants in the test series changed by seven orders of magnitude, and the presence of a strong electron-donating substituent led to the fact that the *cis* form of ArNOO, which is usually inert in bimolecular reactions, was involved into the reaction. Moreover, in the case of nitroso oxide **IIc**, the rate constant for the *cis* form was almost an order of magnitude higher than that for the *trans* form. The dependence of the logarithm of the rate constant on the σ constants of substituents in nitroso oxide molecule on the Hammett scale for *trans* isomers was linear ($r = 0.97$) with a high value of the reaction parameter $\rho = -7 \pm 1$ (Fig. 3). Thus, arylnitroso oxides behave as typical nucleophiles in the reaction with an electron-deficient coreactant,

On the example of nitroso oxide **IIc**, we studied the effect of the polarity of a medium on the kinetics of the reaction under study. The reaction rate constants of the *cis* and *trans* forms of this nitroso oxide with TCE in hexane were $(2.3 \pm 0.2) \times 10^4$ and $(4.4 \pm 0.2) \times 10^6$ L mol^{-1} s^{-1}, respectively. That is, the inversion of the reactivity of the **IIc** isomers occurred in a nonpolar medium: the reaction rate constant for *trans*-**IIc** increased by almost an order of magnitude and, on the contrary, the rate constant for *cis*-**IIc** decreased by two orders of magnitude (Table 1).

Quantum-Chemical Study of the Reaction Mechanism

A detailed study of the mechanism of nitroso oxide reactions with tetracyanoethylene was carried out using the density functional theory in the M06L/6-311+G(d, p) + IEFPCM approximation (solvent: acetonitrile (MeCN)), which adequately describes the geometric characteristics of aromatic nitroso oxides

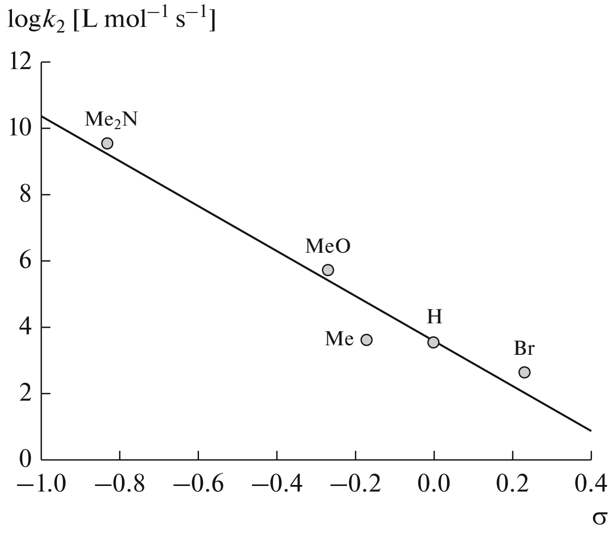

Fig. 3. Dependence of the reaction rate constants of the *trans* forms of nitroso oxides with TCE on the electronic properties of substituents according to the Hammett equation ($T = 295 \pm 2$ K).

Table 2. Enthalpy and Gibbs energy of formation of prereaction complex **III**, activation thermodynamic parameters of two reaction pathways of arylnitroso oxides with TCE (kJ/mol), and key geometrical characteristics of the structures studied (Å)*

4-R-ArNOO	III					TS1					TS2				
	r(C–O)	*r*(C–N)	*r*(O–O)	ΔH°	ΔG°	*r*(C–O)	*r*(C–N)	*r*(O–O)	$\Delta H^{\neq}$	$\Delta G^{\neq}$	*r*(C–O)	*r*(C–N)	*r*(O–O)	$\Delta H^{\neq}$	$\Delta G^{\neq}$
cis															
H	2.695	3.280	1.346	–20.3	19.8	1.803	4.741	1.572	37.5	43.7	1.661	2.934	1.455	41.9	54.7
Br	2.662	3.230	1.348	–20.1	22.9	1.792	4.734	1.551	34.3	34.7	1.658	2.994	1.458	37.9	46.1
Me	2.653	3.224	1.352	–23.2	20.2	1.796	4.725	1.544	30.0	30.9	1.667	2.992	1.460	35.2	43.8
MeO	2.591	3.221	1.362	–27.8	16.9	1.800	4.721	1.518	23.5	26.5	1.684	3.143	1.469	26.1	33.5
Me_2N	2.441	3.180	1.373	–40.9	6.5	1.828	4.683	1.483	11.9	14.1	1.737	3.161	1.456	12.4	16.2
trans															
H	2.608	2.940	1.327	–23.6	18.4	1.690	4.383	1.455	47.3	51.6	1.687	2.598	1.379	25.6	38.8
Br	2.593	2.947	1.329	–23.1	17.8	1.694	4.406	1.442	42.6	47.9	1.698	2.633	1.379	22.7	33.7
Me	2.545	2.932	1.334	–26.7	14.9	1.706	4.410	1.443	38.8	43.8	1.688	2.643	1.383	20.7	33.4
MeO	2.440	2.903	1.344	–32.3	12.5	1.739	4.441	1.429	28.6	31.3	1.701	2.715	1.386	13.1	22.0
Me_2N	2.346	2.928	1.356	–47.1	1.1	1.803	4.486	1.415	15.5	16.3	1.737	2.833	1.390	3.4	8.5

* Figure 4 shows the structures of the test compounds using nitroso oxide **IIb** as an example. The enthalpy and Gibbs energy of complex **III** were calculated relative to the sum of the enthalpies and Gibbs energies of the reactants, and the activation thermodynamic parameters were calculated relative to **III**.

and the activation parameters of the conformational and irreversible transformations of ArNOO [15, 16].

A one-center attack of the terminal oxygen atom of nitroso oxide on a carbon atom of the double bond of TCE can be a possible reaction path for the interaction of reactants. Figure 4 shows the transition state (TS) TS1 corresponding to this reaction channel based on the example of the addition of the *cis* isomer of **IIb**. The structure of TS1 essentially depends on the nature of the substituent in ArNOO (Table 2); nevertheless, the general regularity of the interaction, which consists in a noticeable elongation of the O–O bond in TS1, can be noted. Indeed, the scanning of the PES along the intrinsic reaction coordinate for both *cis*- and *trans*-ArNOO indicated the peroxide bond breakdown in the valley of the reaction products, which are obviously epoxide **IV** and corresponding *para*-substituted nitrosobenzene **V**. Table 2 summarizes the key geometric characteristics and changes in the enthalpy and free Gibbs energy for the studied transformations (Fig. 4 shows the structure of nitroso oxide **IIb** and key structures on the PES of the reaction).

A thorough study of the potential energy surface of the reacting system allowed us to find that pre-reaction complexes **IIIa**–**IIIe** can also be formed in the course of the interaction of the *cis* and *trans* isomers of nitroso oxides **IIa**–**IIe** with tetracyanoethylene. These complexes were stabilized due to partial electron-density transfer from nitroso oxide to the olefin: from 0.260/0.267 electron units for *cis/trans*-**IIa** to 0.464/0.471 electron units for *cis/trans*-**IIb** (Mulliken analysis). The structure of this complex (Fig. 4) is favorable for the occurrence of the two-center addition of ArNOO to the double bond of TCE ([3 + 2]-cycloaddition). It should be noted that the interaction of this type is most characteristic of the reactions of aromatic nitroso oxides with alkenes [17, 18]. However, the interaction of ArNOO with electron-deficient TCE has its own distinctive features. The localization of the transition state of the formally two-center addition of ArNOO to TCE leads to a structure in which the C–O bond is almost formed, whereas the C–N interatomic distance is 2.6–2.8 Å for *trans*-ArNOO or 2.9–3.2 Å for the *cis* isomer (Fig. 4 for *trans*-TS2**b** and Table 2). The TS structure is radically different from the geometrical parameters of the transition states of the interaction of PhNOO with ethylene, propene [18], and 1-hexene [17], for which the C$\cdots$O and C$\cdots$N interatomic distances are approximately the same.

An interesting feature of this reaction path is that the dynamics of the reaction system after overcoming TS2 was different for the *cis* and *trans* isomers of ArNOO. Thus, the PES scanning of the *cis*-ArNOO + TCE system along the intrinsic reaction coordinate indicated that the *cis*-TS2 was further transformed into epoxide **IV** and *para*-substituted nitrosobenzene **V** (Scheme 2).

Reaction of aromatic nitroso oxides with tetracyanoethylene

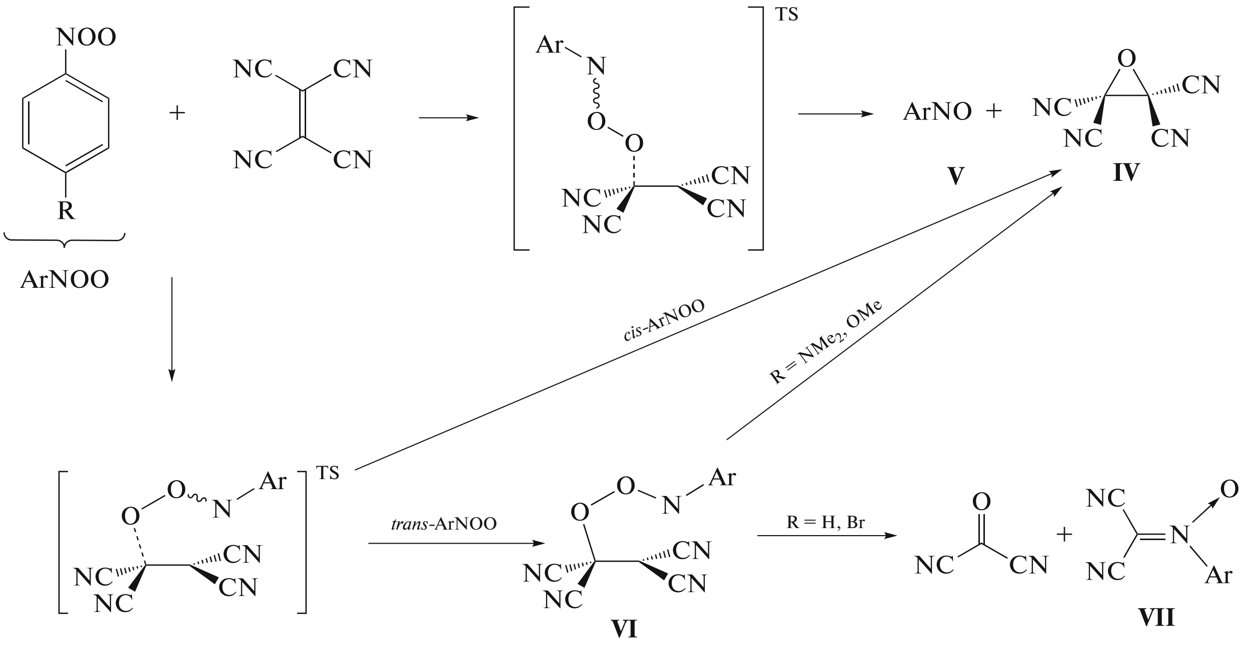

Scheme 2.

In the case of the *trans* isomer of ArNOO, metastable intermediate **VI** (a single-center addition product) was formed after overcoming the saddle point of the PES (Fig. 4). The study of possible further transformations of this intermediate revealed the occurrence of parallel channels for the decay of **VI**. One of them, through the transition state TS3 (Fig. 4), led to an unstable five-membered ring, which spontaneously decomposed into dicyanocarbonyl $OC(CN)_2$ and nitrone **VII** in accordance with the reaction scheme (Scheme 2). In general, this direction of the reaction of *trans*-ArNOO with TCE can be classified as asynchronous [3 + 2]-cycloaddition. Note that the activation energy of the second stage of [3 + 2]-cyclization strongly depends on the nature of the substituent in ArNOO (Table 3), and a significant activation barrier TS3 should be overcome in the case of arylnitroso oxides with electron-donating substituents. Alternatively, intermediate **VI** can undergo the O–O bond cleavage to form products **IV** and **V**. This reaction channel is characterized by a free activation energy of ~30 kJ/mol, regardless of the electronic properties of substituents in the starting nitroso oxide. Figure 4 shows the structure of the transition state TS4**b**, and Table 3 summarizes the most important geometry and energy parameters of the reaction.

An analysis of the energetics of the studied transformations in general allowed us to propose an overall scheme of the reaction for the interaction of aromatic nitroso oxides with tetracyanoethylene (Scheme 2), according to which the *cis* and *trans* isomers of ArNOO react differently, and the electronic properties of the *para* substituent affect significantly the reaction mechanism. Thus, *cis*-ArNOO are more reactive than the *trans* isomers if the single-center nucleophilic addition of ArNOO to TCE is realized through the transition state TS1 (Table 2). A significant decrease in the activation barrier upon the introduction of an electron-donating substituent into ArNOO explains the experimentally observed high reactivity of the *cis* isomers of 4-Me_2N- and 4-MeO-substituted arylnitroso oxides. The results of our calculations allowed us to estimate the rate constants k_2 for the other *cis*-ArNOO as $\leq 10^3$ L mol^{-1} s^{-1}, which did not allow us to reliably detect an increase in the effective rate constant k_{eff} in the presence of the TCE additives at the used concentrations of olefin (10^{-3}–10^{-4} mol/L).

The situation changed in the study of the reactivity of the *trans* isomers of ArNOO. First, the rate constants k_1 for the *trans* isomers are much lower (Table 1) than those for *cis*-ArNOO; this allowed us to reliably fixate the growth of the effective rate constant $k_{eff} = k_1 + k_2[TCE]$ with increasing tetracyanoethylene concentration and thus to determine the bimolecular rate constants k_2 of 10^2 L mol^{-1} s^{-1} or more upon the introduction of the TCE additives of about 10^{-3} mol/L (Fig. 1). Second, the *trans* isomers of ArNOO are more active than the *cis* isomers on the realization of the formally two-center reaction mechanism with the TS2 saddle point (Table 2), and the energy of TS2 is comparable to the energy of TS1 for both ArNOO isomers. Hence, it follows that the absolute reactivity of the *cis*- and *trans*-ArNOO isomers in the reaction with TCE is approximately the same, as it was observed experimentally for nitroso oxides **IIb** and **IIc** (Table 1). Third, the transition state TS2 is converted into metastable intermediate **VI**, the subsequent transformation

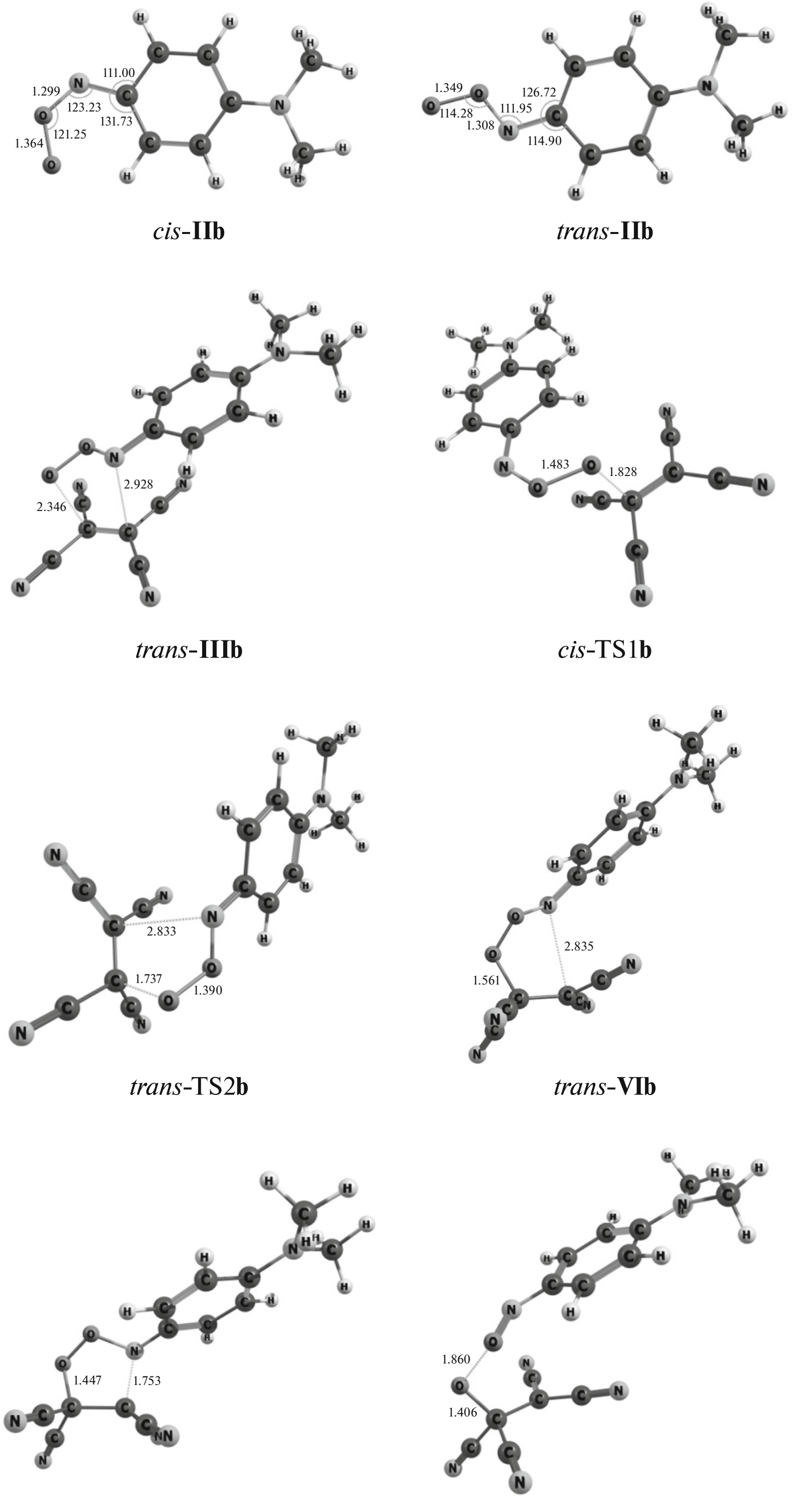

cis-**IIb** *trans*-**IIb**

trans-**IIIb** *cis*-TS1**b**

trans-TS2**b** *trans*-**VIb**

trans-TS3**b** *trans*-TS4**b**

Fig. 4. The structures of a nitroso oxide (**IIb**), its complex with TCE (**IIIb**), an intermediate (**VIb**), and the transition states of various channels of the reaction of **IIb** with TCE (TS1**b**–TS4**b**). The bond lengths and bond angles are given in angstrom units and degrees, respectively.

Table 3. Enthalpy and Gibbs energy of formation of intermediate **VI**, activation thermodynamic parameters of two paths of **VI** decay, and key geometric characteristics of the studied structures*

4-R-ArNOO	VI					TS3					TS4				
	r(C–O)	r(C–N)	r(O–O)	$\Delta H°$	$\Delta G°$	r(C–O)	r(C–N)	r(O–O)	$\Delta H^{\neq}$	$\Delta G^{\neq}$	r(C–O)	r(C–N)	r(O–O)	$\Delta H^{\neq}$	$\Delta G^{\neq}$
	Å			kJ/mol		Å			kJ/mol		Å			kJ/mol	
trans-															
H	1.557	2.518	1.403	1.6	–0.2	1.474	1.987	1.415	7.7	13.0	1.412	2.829	1.809	32.2	29.9
Br	1.558	2.568	1.403	1.6	1.4	1.469	1.964	1.416	12.3	19.1	1.410	2.867	1.815	32.9	32.1
Me	1.569	2.589	1.403	2.0	–1.2	1.466	1.937	1.418	17.0	25.0	1.413	2.876	1.815	32.1	32.7
MeO	1.576	2.669	1.405	1.9	2.1	1.458	1.865	1.420	32.3	37.3	1.411	2.935	1.825	32.2	29.6
Me_2N	1.561	2.835	1.415	1.2	0.1	1.447	1.753	1.424	68.5	75.7	1.406	3.043	1.860	31.8	30.5

* Figure 4 shows the structures of the studied compounds using nitroso oxide **IIb** as an example. The enthalpy and Gibbs energy of intermediate **VI** were calculated relative to TS2, and those of the transition states TS3 and TS4, relative to **VI**.

of which depends on the electronic properties of the *para* substituent. A comparison of the activation barriers of TS3 and TS4 indicated that, in the presence of strong electron-donating substituents in *trans*-ArNOO, intermediate **VI** preferentially disintegrated at the peroxide bond must. Otherwise, the cyclization of **VI** according to Scheme 2 is likely.

Thus, the results of a theoretical study suggest that substituted nitrosobenzene **V** and tetracyanooxirane **IV** are the only reaction products of nitroso oxides **IIb**, **IIe**, and possibly **IId** (Scheme 2). Nitroso oxides **IIa** and **IIe** give a more complex mixture of products because dicyanocarbonyl and nitrone **VII** result from the interaction of the *trans* isomer with TCE in addition to compounds **IV** and **V** (*cis*-ArNOO reaction products). The products of ArNOO reactions with TCE are under study in our laboratory.

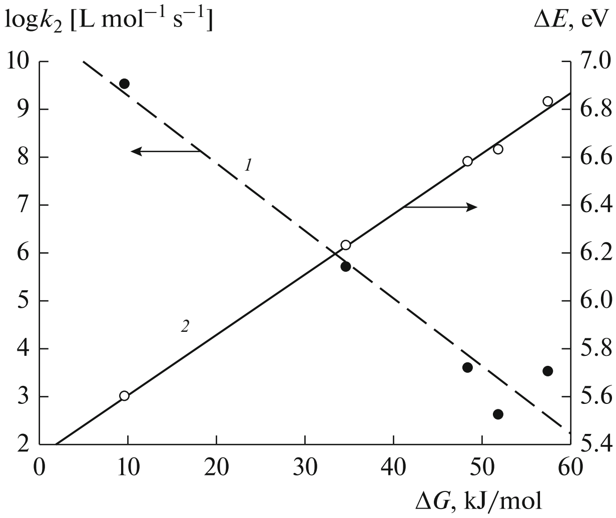

Fig. 5. (*1*) Correlation of the Gibbs activation energy ΔG calculated in the M06L/6-311+G(d,p) + IEFPCM approximation (solvent: MeCN) and the experimentally observed rate constant of the reaction of the *trans* isomer of ArNOO with TCE; (*2*) relationship between ΔG and the value of $\Delta E = E(\text{ArNOO}^{\bullet +}) - E(\text{ArNOO})$, which characterizes the nucleophilic properties of nitroso oxide in acetonitrile.

In general, an excellent agreement between experimental and calculated data was observed. Figure 5 shows a correlation between the calculated Gibbs activation energies $\Delta G = G(\text{TS2}) - G(\text{ArNOO}) - G(\text{TCE})$ and the logarithm of the rate constants k_2 for the reactions of *trans*-ArNOO with TCE. The found electronic effects of the reaction were confirmed by the calculation: the vertical ionization energy of nitroso oxide in a MeCN solvent $\Delta E = E(\text{ArNOO}^{\bullet +}) - E(\text{ArNOO})$ was used as a measure of the nucleophilicity of ArNOO. As can be seen in Fig. 5, there is an excellent correlation between the values of ΔG and ΔE, which fully confirms the conclusion made based on the Hammett correlation (Fig. 3) on the nucleophilic nature of the interaction of aromatic nitroso oxides with tetracyanoethylene. The above regularities of changes in the geometric characteristics (Tables 2 and 3) and electron density distributions in the ArNOO···TCE complexes and transition states are also consistent with the nucleophilic mechanism of the reaction.

CONCLUSIONS

Thus, we found that aromatic nitroso oxides exhibit nucleophilic nature in the reaction with tetracyanoethylene. In the presence of a strong electron-donating substituent (Me_2N or MeO) the *para* position of the aromatic ring, the *cis* form of nitroso oxide, which is usually inert toward organic substrates, reacts with TCE along with the *trans* form. We studied the reaction mechanism using density functional theory methods. We found that the mechanism was different for the *cis* and *trans* isomers, and they essentially depended on the nature of substituents in the aromatic ring of ArNOO. The *cis* isomers are more reactive than the *trans* isomers in the single-center nucleophilic addition to the olefin. The activation barrier of reaction significantly decreased in the presence of an electron-donating substituent in *cis*-ArNOO; this fact is consistent with the experimental results. The *trans* isomers are more active than the *cis* isomers if the reaction proceeds through asynchronous [3 + 2]-cycloaddition, which results in the formation of a metastable intermediate, and the direction of the decay of this intermediate is determined by the nature of the substituent in the aromatic ring of nitroso oxide.

ACKNOWLEDGMENTS

The theoretical and experimental studies were carried out using the equipment of the Chemistry Center for Collective Use at the Ufa Institute of Chemistry of the Ufa Research Center of the Russian Academy of Sciences.

REFERENCES

1. Gritsan, N.P., *Russ. Chem. Rev.*, 2007, vol. 76, no. 12, p. 1139.
2. Chainikova, E.M., Khursan, S.L., and Safiullin, R.L., *The Chemistry of Peroxides*, Greer, A. and Liebman, J.F., Ed., Chichester, UK: John Wiley & Sons Ltd., 2014, vol. 3, p. 357.
3. Khursan, V.S., Kovaleva, O.A., Chainikova, E.M., Talipov, M.R., and Safiullin, R.L., *High Energy Chem.*, 2010, vol. 44, no. 4, p. 284.
4. Chainikova, E.M., Safiullin, R.L., Faizrakhmanova, I.M., and Galkin, E.G., *Kinet. Catal.*, 2009, vol. 50, no. 2, p. 174.
5. Lindsay, R.O. and Allen, G.F.H., *Org. Synth.*, 1955, vol. 3, p. 710.
6. Smith, P.A.S. and Boye, J.H., *Org. Synth.*, 1963, vol. 4, p. 75.
7. Maslennikov, S.I., Nikolaev, A.I., and Komissarov, V.D., *Kinet. Katal.*, 1979, vol. 20, no. 2, p. 326.
8. Zhao, Y. and Truhlar, D.G., *J. Chem. Phys.*, 2006, vol. 125, p. 194101.
9. McLean, A.D. and Chandler, G.S., *J. Chem. Phys.*, 1980, vol. 72, p. 5639.
10. Raghavachari, K., Binkley, J.S., Seeger, R., and Pople, J.A., *J. Chem. Phys.*, 1980, vol. 72, p. 650.
11. Frisch, M.J., Trucks, G.W., Schlegel, H.B., Scuseria, G.E., Robb, M.A., Cheeseman, J.R., Scalmani, G., Barone, V., Mennucci, B., Petersson, G.A., Nakatsuji, H., Caricato, M., Li, X., Hratchian, H.P., Izmaylov, A.F., Bloino, J., Zheng, G., Sonnenberg, J.L., Hada, M., Ehara, M., Toyota, K., Fukuda, R., Hasegawa, J., Ishida, M., Nakajima, T., Honda, Y., Kitao, O., Nakai, H., Vreven, T., Montgomery, J.A., Peralta, J.E., Ogliaro, F., Bearpark, M., Heyd, J.J., Brothers, E., Kudin, K.N., Staroverov, V.N., Kobayashi, R., Normand, J., Raghavachari, K., Rendell, A., Burant, J.C., Iyengar, S.S., Tomasi, J., Cossi, M., Rega, N., Millam, J.M., Klene, M., Knox, J.E., Cross, J.B., Bakken, V., Adamo, C., Jaramillo, J., Gomperts, R., Stratmann, R.E., Yazyev, O., Austin, A.J., Cammi, R., Pomelli, C., Ochterski, J.W., Martin, R.L., Morokuma, K., Zakrzewski, V.G., Voth, G.A., Salvador, P., Dannenberg, J.J., Dapprich, S., Daniels, A.D., Farkas, O., Foresman, J.B., Ortiz, J.V., Cioslowski, J., and Fox, D.J., *Gaussian 09*, Wallingford, CT: Gaussian Inc., 2009.
12. Tomasi, J., Mennucci, B., and Cammi, R., *Chem. Rev.*, 2005, vol. 105, p. 2999.
13. Simon, S., Duran, M., and Dannenberg, J.J., *J. Chem. Phys.*, 1996, vol. 105, p. 11024.
14. Chainikova, E.M., Khursan, S.L., and Safiullin, R.L., *Kinet. Catal.*, 2006, vol. 47, no. 4, p. 549.
15. Yusupova, A.R., Safiullin, R.L., and Khursan, S.L., *J. Chem. Phys. A*, 2016, vol. 120, no. 28, p. 5693.
16. Chainikova, E.M., Yusupova, A.R., Khursan, S.L., Teregulova, A.N., Lobov, A.N., Abdullin, M.F., Enikeeva, L.V., Gubaydullin, I.M., and Safiullin, R.L., *J. Org. Chem.*, 2017, vol. 82, no. 15, p. 7750.
17. Talipov, M.R., Khursan, S.L., and Safiullin, R.L., *Khim. Fiz.*, 2009, vol. 28, no. 7, p. 17.
18. Talipov, M.R., Khursan, S.L., and Safiullin, R.L., *Russ. J. Phys. Chem. A*, 2011, vol. 85, no. 3, p. 364.

Translated by V. Makhlyarchuk